ters 15, 300 (1965).
[16]E. W. Schmid, Y. C. Tang, and K. Wildermuth, Phys. Letters 7, 263 (1963).
[17]K. Wildermuth and W. McClure, in *Cluster Representations of Nuclei, Springer Tracts in Modern Physics*, edited by G. Höhler (Springer-Verlag, Berlin, Germany, 1966), Vol. 41.
[18]D. W. Devins, S. M. Bunch, H. H. Forster, J. Hokhikian, and C. C. Kim, Nucl. Phys. A126, 261 (1969).
[19]W. K. Lin, F. Scheibling, and R. W. Kavanagh, Phys. Rev. C 1, 816 (1970).
[20]T. Harper, I. Inouye, and N. C. Rasmussen, Nucl. Instr. Methods 67, 125 (1969).
[21]L. D. Pearlstein, Y. C. Tang, and K. Wildermuth, Phys. Rev. 120, 224 (1960); D. R. Thompson, I. Reichstein, W. McClure, and Y. C. Tang, Phys. Rev. 185, 1351 (1969).
[22]P. Darriulat, D. Garreta, A. Tarrats, and J. Testoni, Nucl. Phys. A108, 316 (1968); S. N. Bunker, J. M. Cameron, M. B. Epstein, G. Paić, J. R. Richardson, J. G. Rogers, P. Tomas, and J. W. Verba, Nucl. Phys. A133, 537 (1969).
[23]D. K. Olsen and R. E. Brown, Phys. Rev. 176, 1192 (1968).
[24]V. Valkovic, C. Joseph, S. T. Emerson, and G. C. Phillips, Nucl. Phys. A106, 138 (1968).
[25]A. S. Wilson, M. C. Taylor, J. C. Legg, and G. C. Phillips, Nucl. Phys. A130, 624 (1969).
[26]D. Daronian, J. C. Faivre, D. Garreta, J. Goudergues, J. Jungerman, H. Krug, B. Mayer, A. Pages, A. Papineau, and J. Testoni, Nucl. Phys. A104, 111 (1967).
[27]J. D. Seagrave, in *Three-Body Problem in Nuclear and Particle Physics*, edited by J. S. C. McKee and P. M. Rolph (North-Holland Publishing Company, Amsterdam, The Netherlands, 1970), p. 41.
[28]W. Haeberli, in *Three-Body Problem in Nuclear and Particle Physics*, edited by J. S. C. McKee and P. M. Rolph (North-Holland Publishing Company, Amsterdam, The Netherlands, 1970), p.188.
[29]W. T. H. van Oers and K. W. Brockman, Jr., Nucl. Phys. 92, 561 (1967).
[30]W. Ebenhöh, A. S. Rinat-Reiner, and Y. Avishai, Phys. Letters B29, 638 (1969).

PHYSICAL REVIEW C VOLUME 3, NUMBER 5 MAY 1971

Strong-Interaction Effects in K-Mesonic Atoms*

William A. Bardeen and E. Wayne Torigoe†
Institute of Theoretical Physics, Department of Physics, Stanford University, Stanford, California 94305
(Received 13 January 1971)

The process of absorption in K-mesonic atoms is studied with special emphasis on the role of the $Y_0^*(1405)$ resonance. An effective t-matrix method is developed to incorporate the effects of the resonance. Detailed calculations of the absorption process, based on an independent-particle model of the nucleus, were made for selected nuclei. The results of these calculations are compared with available x-ray and emulsion data for moderate to heavy nuclei.

I. INTRODUCTION

While electron scattering experiments[1] and the study of muonic atoms[2] provide effective means of acquiring detailed information on proton distributions, simple probes of the neutron distribution have yet to be found. The scattering of hadrons off nuclei can be used to study nuclear structure and average nuclear properties, but isolation of the neutron distribution requires interpretation of many types of experimental results. In the study of pionic atoms,[3] absorption of protons and neutrons may be distinguished, but the absorption requires two nucleons, resulting in a strong dependence on nuclear correlations.

Although techniques for directly measuring the entire neutron distribution in nuclei do not exist, the study of K-mesonic atoms was proposed by Wilkinson[4] as an effective probe of nucleon densities in the nuclear periphery. Calculations by Jones[5] indicated that the K meson would be largely trapped in circular orbits during the electronic cascade prior to absorption in the nuclear surface. On the basis of the position of the K-meson–proton overlap for these orbits, as shown for a typical case in Fig. 1, the absorption of K mesons is expected to take place in the low-density region at the nuclear surface. Unlike the absorption in π-mesonic atoms, absorption on single nucleons is possible via the open inelastic channels

$$\begin{aligned} &K^- + p \to \Sigma^+ + \pi^-, \Sigma^0 + \pi^0, \Sigma^- + \pi^+, \Lambda + \pi^0, \\ &K^- + n \to \Sigma^0 + \pi^-, \Sigma^- + \pi^0, \Lambda + \pi^-, \end{aligned} \tag{1}$$

which release sufficient energy to overcome even the largest possible binding energies of the nucleon and K meson. Thus, with appropriate information on the rates for these reactions, the nucleon densities in the nuclear periphery, to a first approximation, are directly given by measurements of absorption rates in K-mesonic atoms. Following this initial description of the absorption pro-

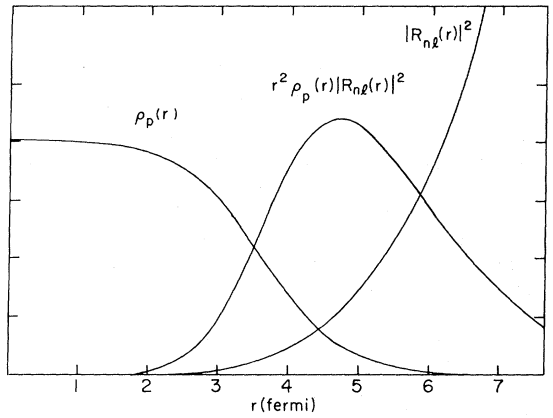

FIG. 1. Radial overlap for ^{40}Ca. The K-meson radial wave function corresponds to $l = n - 1 = 3$. The proton density is a Fermi distribution with $R = 3.602$ F and $a = 0.576$ F [see Eq. (35)].

cess by Wilkinson and Jones, other authors have elaborated on the electronic cascade and the effect of motion of the nucleons.[6]

After these early discussions, several studies of K-mesonic atoms were undertaken to resolve questions related to the neutron density at the surface of nuclei. On the basis of emulsion experiments, Davis *et al.*,[7] Burhop,[8] and Burhop *et al.*[9] have concluded that a large neutron excess exists in the periphery of heavy nuclei. This was also claimed by Wiegand[10] in an analysis of x-ray data for K-mesonic atoms. On the other hand, Bugg *et al.*[11] and Ericson[12] have argued that this neutron excess is not required to interpret the observations. In these investigations the interaction between the K meson and the nucleus was described using optical-model potentials or constant scattering lengths fitting above threshold K^--p scattering data. Unfortunately, as noted by Bloom, Johnson, and Teller,[13] the K^--p resonance at 1405 MeV lies well within the range of energies involved in K-mesonic absorption. As shown in the following analysis, the effectiveness of the study of K-mesonic atoms in determining the neutron density is markedly reduced by the resonance.

In this paper we present a description of the absorption of bound K mesons on moderate to heavy nuclei which takes into account the effects of the K^--p resonance. An analysis of the absorption using a simple pseudopotential method is given in Sec. II. With this approach, the importance of properly treating the resonance effects is demonstrated. In Sec. III the resonance effects are incorporated in the description of the absorption using an effective scattering matrix. This is followed in Sec. IV by a discussion of approximations which allow an independent-particle shell-model description of the nucleus to be utilized in evaluating absorption rates. Calculations based on this type of nuclear model were performed for ^{16}O, ^{40}Ca, and ^{96}Mo and are compared with observations in Secs. V and VI. In Sec. V the extraction of information on neutron distributions from K-mesonic x-ray spectra is examined, and in Sec. VI, predictions concerning momentum distributions, opening-angle distributions, and branching ratios are compared with the results of emulsion and bubble-chamber experiments.

II. PSEUDOPOTENTIAL METHOD

As a first approximation to a description of K-mesonic absorption, we use a simple pseudopotential model to describe the K-meson–nucleon interaction. Near the K-nucleon threshold the interaction is predominately S wave. Hence we construct a pseudopotential which in the Born approximation gives the correct S-wave K^--nucleon amplitude.

$$V_{KN}(\vec{x}-\vec{y}) = (U - iW)\delta(\vec{x}-\vec{y}). \tag{2}$$

With this potential, the center-of-mass scattering amplitude is given by

$$f_{KN} = -\frac{1}{4\pi}\frac{2\mu}{\hbar^2}\int d^3x\, e^{-i\vec{k}'\cdot\vec{x}} V_{KN}(x)\, e^{i\vec{k}\cdot\vec{x}}$$

$$= -\frac{1}{4\pi}\frac{2\mu}{\hbar^2}(U - iW), \tag{3}$$

where μ is the reduced mass, $\mu = M_K M_N/(M_K + M_N)$. Inverting Eq. (3), we have the result

$$-U + iW = 4\pi(\hbar^2/2\mu) f_{KN}. \tag{4}$$

The pseudopotential is complex because of the open inelastic channels.

The K-nucleus pseudopotential is constructed as a sum of two-body potentials.

$$V_{KA} = \sum_i (U_i - iW_i)\delta(\vec{x}-\vec{y}_i), \tag{5}$$

where the sum ranges over all nucleons with the potential strength different for neutrons and protons. The effective potential seen by the K meson may be found by taking the matrix element of the potential in Eq. (5) in the nuclear ground state. The resulting potential is

$$V_{KA}(\vec{x}) = (U_p - iW_p)\rho_p(\vec{x}) + (U_n - iW_n)\rho_n(\vec{x}), \tag{6}$$

where $\rho_p(\vec{x})$ and $\rho_n(\vec{x})$ are the proton and neutron densities, respectively.

In lowest-order perturbation theory, the energy shift and the absorption rate for a K meson in a definite atomic (n, l) orbit are given by

$$\Delta E_{nl} - \tfrac{1}{2}i\hbar\Gamma_{nl} = \langle nl|V_{KA}|nl\rangle,$$

$$= \frac{1}{4\pi}\int d^3x\, V_{KA}(\vec{x})|R_{nl}(x)|^2, \tag{7}$$

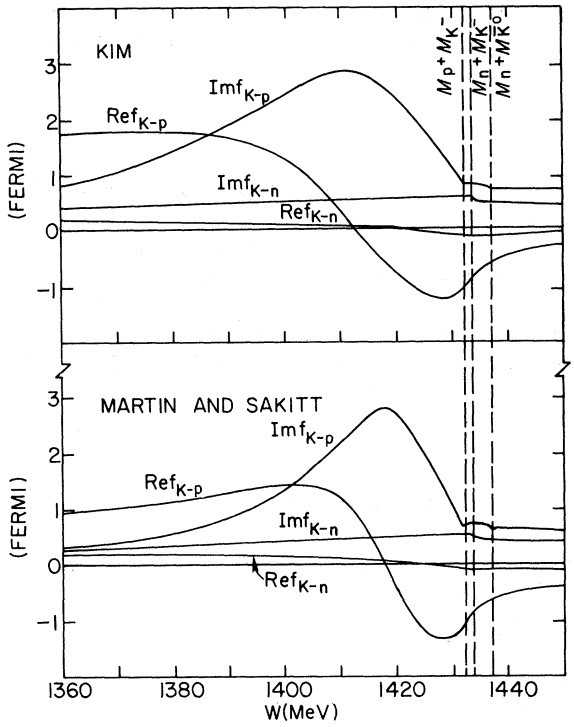

FIG. 2. Real and imaginary parts of the scattering amplitudes for the $\bar{K}$-nucleon interaction versus center-of-mass energy.

where $R_{nl}(x)$ is the normalized radial wave function for the K meson. Thus the energy shift and absorption rate are given by

$$\Delta E_{nl}=\frac{1}{4\pi}\int d^3x[U_p\rho_p(\vec{x})+U_n\rho_n(\vec{x})]|R_{nl}(x)|^2,$$
$$\Gamma_{nl}=\frac{1}{4\pi\hbar}\int d^3x[2W_p\rho_p(\vec{x})+2W_n\rho_n(\vec{x})]|R_{nl}(x)|^2. \quad (8)$$

The above relations would allow us, in principle, to determine the nucleon densities from the x-ray data if unique values for the pseudopotential parameters existed. The pseudopotential parameters are directly related to the K^--nucleon S-wave scattering amplitudes using Eq. (4). In Fig. 2 we show the results of fits to the data by Kim[14] and by Martin and Sakitt.[15] In both fits the K^--neutron amplitude is slowly varying at all energies. However, the K^--proton amplitude is rapidly varying below threshold because of the presence of the $Y_0^*(1405)$ resonance in this channel. Thus in order to determine the proton pseudopotential parameter, we must examine the energy available in the center of mass of the K^--proton system during absorption.

Neglecting the K-meson binding energy, we have from energy conservation

$$E\simeq M_K+M_p-\epsilon_p-P^2/2(M_K+M_p), \quad (9)$$

where ϵ_p is the binding energy of the absorption proton and P is the total momentum of the absorption products. The range of proton binding energies in nuclei is comparable with the width of the K^--proton resonance peak, but since absorption largely occurs in the nuclear periphery, absorption on lightly bound nucleons will be somewhat favored. Thus, a reasonable range for proton binding energies involved in absorption is 8 to 15 MeV.

The range of values expected for the kinetic energy term may be roughly estimated by considering the K-proton overlap as a wave function describing the motion of the center of mass of the absorption products in the absence of interactions with the residual nucleus. Since spherical Bessel functions represent free-particle states with definite momentum and angular momentum magnitudes, the momentum distribution for absorption products with total angular momentum j is given by

$$\frac{dN}{dP}(P)\propto P^2\left[\int_0^\infty dr\, r^2 j_j(Pr)\rho_p^{1/2}(r)R_{l+1,l}(r)\right]^2, \quad (10)$$

where $\rho_p(r)$ is the proton density and $R_{l+1,l}$ is the radial wave function for the K-mesonic orbit from which absorption takes place.

Since the total angular momentum of the absorption products is given by the sum of the K-meson and absorption-nucleon angular momenta, the momentum distribution of absorption products is comprised of a linear combination of distributions given by Eq. (10), taken over all possible j values. The angular momentum of the K meson at absorption is generally larger than that of the nucleon, which may take on several values. Thus, possible j values will be centered about the K-meson angular momentum. As a rough approximation to the momentum distribution, we use Eq. (10) with j equal to l. This procedure essentially neglects the angular momentum of the nucleons. However, since the introduction of additional j values on both sides of l should primarily broaden the distribution, we expect the average kinetic energy derived from this distribution to be roughly correct.

Since absorption occurs in the low-density region of the nucleus, we can approximate the proton density by

$$\rho(r)\propto e^{-2\beta r},$$

where $1/2\beta$ is the skin-thickness parameter in the case of a Fermi distribution. Substituting l for j and neglecting the exponential dependence of the K-meson wave function, we obtain, from Eq. (10),

$$\frac{dN}{dP}(P)\propto P^{2l+2}/(P^2+\beta^2)^{2l+4}, \quad (11)$$

which peaks at

$$P=\beta(l+1)^{1/2}/(l+3)^{1/2}. \tag{12}$$

The kinetic energy distribution shown in Fig. 3 corresponds to this momentum distribution evaluated for the parameters used in Fig. 1.

From Fig. 3 we see that the kinetic energy ranges from about 3 to 15 MeV. Hence, adding the binding-energy contribution, the K-p center-of-mass energy varies from about 10 to 30 MeV below threshold, i.e., from about 1400 to 1420 MeV. This is just the region where resonance effects are strongest and the real part of the K-p amplitude is most rapidly varying. The range of energies is comparable with the width of the resonance, preventing specification of an accurate proton pseudopotential, especially for the fit by Martin and Sakitt. In the next section an analysis of the absorption which includes an energy-dependent treatment of the K-nucleon interaction is presented.

III. EFFECTIVE SCATTERING MATRIX ANALYSIS

The pseudopotential analysis discussed in Sec. II fails to describe the K-meson absorption process, as it cannot account for the rapid variation of the K^--proton scattering amplitude with energy. In this section, we consider a generalization of the pseudopotential method which involves the construction of an effective scattering matrix to describe the absorption.

We want to construct a model to calculate the transition rate for a K^- meson in a given electronic orbit to a final state containing a hyperon, a pion, and a residual nucleus, $K^-(nl)+A \to Y'+\pi'+A'$.

We can express the transition rate Γ in terms of the production matrix element of the scattering operator, $R=S-1$,

$$d\Gamma=\frac{1}{T}|\langle A', Y', \pi'|R|A, K^-(nl)\rangle|^2 df. \tag{13}$$

Our model for the R matrix is based on the following three assumptions:
(a) Absorption occurs on single nucleons.
(b) Only S-wave production is important.
(c) Off-shell extrapolations are neglected.
Using these assumptions, we can write the production R matrix in terms of the hadron fields

$$R=\int dx \int dy\; Y^+(x)\pi(x)G(x-y)N(y)K^+(y), \tag{14}$$

where we have suppressed the spin and isospin indices. The function $G(x)$ can be identified with the center-of-mass production amplitude, $f^{K^-}(W)$, by taking the matrix element of Eq. (14). We have

$$i\frac{4\pi W}{(M_Y M_N)^{1/2}} f^{K^-}(W)=\int dx\, e^{ip\cdot x}G(x), \tag{15}$$

where $W^2=p^2$. Hence, we can invert Eq. (15) to obtain

$$G(x)\doteq\frac{i}{(2\pi)^4}\int dp\, e^{-ip\cdot x}\frac{4\pi W}{(M_Y M_N)^{1/2}} f^{K^-}(W). \tag{16}$$

Actually, Eq. (16) is only defined in terms of its Fourier transform.

We can use Eqs. (14) and (16) to calculate the absorption matrix elements. If we neglect final-state interactions, we can use plane-wave states for the produced particles. In this case the production matrix element becomes

$$\begin{aligned}\langle A', Y'(p'\sigma'), \pi'(q')|R|A, K^-(nl)\rangle &= \frac{i}{(2\pi)^4}\int dp\left[\int dx\, e^{-ip\cdot x}\frac{e^{ip'\cdot x}}{(2\pi)^{3/2}}\chi^{\sigma'\dagger}\frac{e^{iq'\cdot x}}{(2\pi)^{3/2}}\right]\\ &\times\frac{4\pi W}{(M_Y M_N)^{1/2}} f^{K^-}(W)\left[\int dy\, e^{ip\cdot y}\langle A'|N(y)|A\rangle\frac{V_{nl}(\vec{y})e^{-iE_{nl}y_0}}{(2E_{nl})^{1/2}}\right]\\ &= i(2\pi)^{-3}\frac{4\pi W}{(M_Y M_N)^{1/2}} f^{K^-}(W)\int dy\, e^{i(p'+q')\cdot y}\chi^{\sigma'\dagger}\langle A'|N(y)|A\rangle\frac{V_{nl}(\vec{y})\,e^{-iE_{nl}y_0}}{(2E_{nl})^{1/2}}.\end{aligned} \tag{17}$$

If we neglect the initial-state interactions, then $V_{nl}(\vec{y})$ is simply the electronic wave function for the K meson. A discussion of the approximations involved in neglecting initial- and final-state interactions is given in Sec. V.

We can use Eqs. (13) and (17) to calculate the formal expression for the total transition rate

$$\begin{aligned}\Gamma&=\frac{1}{T}\sum_{A'}\sum_{Y'}\sum_{\pi'}\sum_{\sigma'}\int\frac{d^3p'}{E_{p'}/M_Y}\int\frac{d^3q'}{2\omega_{q'}}|\langle A', Y'(p'\sigma'), \pi'(q')|R|A, K^-(nl)\rangle|^2,\\ &=(2\pi)^{-4}\int d^3p\int d^3x\int d^3y\, e^{i\vec{p}\cdot(\vec{x}-\vec{y})}\int dp_0\int dt\, e^{i(E_{nl}-p_0)t}\langle A|N^\dagger(\vec{x},t)N(\vec{y},0)|A\rangle\\ &\times V_{nl}^*(\vec{x})V_{nl}(\vec{y})\left[\sum_{Y\pi}\frac{Wk^f_{\mathrm{c.m.}}(W)}{E_{nl}M_N}\sigma_{K^-N\to Y\pi}(W)\right].\end{aligned} \tag{18}$$

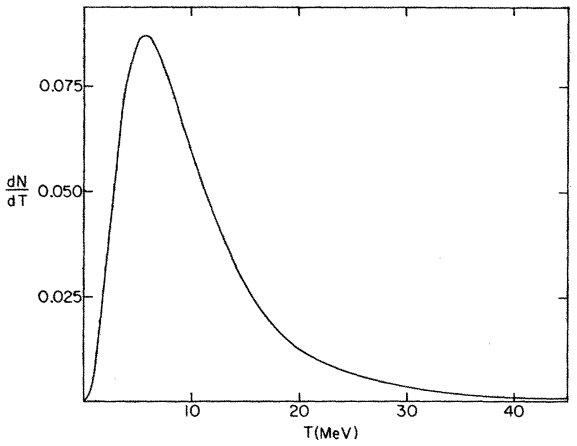

FIG. 3. Kinetic energy distribution for the K-nucleon system calculated from Eq. (11) with $l=3$ and $1/2\beta = 0.576$ F.

In obtaining the final expression in Eq. (18), we have used completeness of the final nuclear states (which are not observed). The center-of-mass momentum of the final state is $k^f_{\text{c.m.}}(W)$, $W^2=p_0{}^2 - p^2$, and $\sigma(W)$ is the appropriate production cross section.

If the hyperon-pion final state is not observed, the optical theorem for the K^--nucleon scattering amplitudes can be used to evaluate the sum over the production cross sections,

$$\sum_{Y\pi} \frac{W k^f_{\text{c.m.}}(W)}{E_{nl} M_N} \sigma_{K^- N \to Y\pi}(W) = \frac{4\pi W}{E_{nl} M_N} \operatorname{Im} f_N^{K^-}(W) . \tag{19}$$

The general expression in Eq. (18) reduces to the results of the pseudopotential calculation if we use a kind of mean-value theorem to replace the amplitude factor of Eq. (19) by a constant. Evaluating the amplitudes at a constant mean energy W^* we have

$$\frac{4\pi W}{E_{nl} M_N} \operatorname{Im} f_N^{K^-}(W) \overset{\text{ave}}{=} \frac{4\pi W^*}{E_{nl} M_N} \operatorname{Im} f_N^{K^-}(W^*) . \tag{20}$$

Using this effective value for the scattering amplitude, we can perform the momentum integrations, and Eq. (18) becomes

$$\begin{aligned} \Gamma = & \int d^3x \langle A | N^\dagger(\vec{x}, 0) N(\vec{x}, 0) | A \rangle | V_{nl}(\vec{x}) |^2 \\ & \times \left[\frac{4\pi W^*}{E_{nl} M_N} \operatorname{Im} f_N^{K^-}(W^*) \right] \\ = & \frac{1}{4\pi} \int d^3x \left[\sum_N \frac{4\pi W^*}{E_{nl} M_N} \operatorname{Im} f_N^{K^-}(W^*) \langle A | \rho_N(\vec{x}) | A \rangle \right] \\ & \times |R_{nl}(x)|^2 , \end{aligned} \tag{21}$$

where $R_{nl}(x)$ is the K-meson radial wave function with

$$V_{nl}(\vec{x}) = R_{nl}(x) Y_{lm}(\hat{x}) .$$

This mean-value calculation of the total absorption rate could, in principle, be used for absorption on both neutrons and protons. However, the strong energy dependence of the proton amplitudes as shown in Fig. 2 precludes an easy estimate of the mean energy W^*. This approach could, however, be used to evaluate absorption on neutrons.

Our subsequent calculations are based on the full expression for the transition rate in Eq. (18). This expression for the transition rate depends on the K^--nucleon production cross sections, the K-meson wave functions, and the ground-state expectation value of the nucleon Green's function. In contrast to the pseudopotential calculation where the transition rate depended only upon the nucleon densities, the effective scattering matrix calculation will, in general, require further knowledge of the nuclear physics embodied in the expectation value of the nucleon Green's function.

IV. INDEPENDENT-PARTICLE APPROXIMATION

An accurate calculation of the absorption rates on protons requires that we include more knowledge of the nuclear state than just the proton density. As the absorption takes place in the low-density region of the nuclear surface (see Fig. 1), typical Fermi models of the nucleons cannot be expected to apply. However, in this low-density region we can expect nuclear correlations to be small, and therefore an independent-particle model of the nucleus should be quite accurate.

The independent-particle approximation means that we can write the ground-state expectation value of the nucleon Green's function in terms of the single-particle wave functions. In this case, we have

$$\langle A | N^\dagger(\vec{x}, t) N(\vec{y}, 0) | A \rangle = \sum_i e^{i(E_A - E_i)t} U_i^*(\vec{x}) U_i(\vec{y}) , \tag{22}$$

where the sum goes over all nucleons, with $U_i(\vec{x})$ being their respective wave functions. We note that the energy difference $E_A - E_i = M_N - \epsilon_i$, where ϵ_i is the binding energy of the nucleon on which absorption occurs.

We can now write the transition rate in terms of the single-particle wave functions.

$$\Gamma = \sum_{Y\pi} \sum_i \int d^3p \, | Z_i(\vec{p}) |^2 \left[\frac{W_i k^f_{\text{c.m.}}(W_i)}{E_{nl} M_N} \sigma_{K^- i \to Y\pi}(W_i) \right] , \tag{23}$$

where the center-of-mass energy W_i is given by $W_i \simeq M_K + M_i - \epsilon_{nl} - \epsilon_i - p^2/2W_i$ with ϵ_{nl} being the K-meson binding energy. The function $Z_i(\vec{p})$ is the Fourier transform of the product of the K-meson wave function and the nucleon wave function,

$$Z_i(\vec{p}) = (2\pi)^{-3/2} \int d^3y\, e^{-i\vec{p}\cdot\vec{y}} U_i(\vec{y}) V_{nl}(\vec{y}) . \quad (24)$$

The important variable which determines the momentum and energy distributions is the total orbital angular momentum of the center-of-mass motion of the K-meson–nucleon system. The momentum distributions can be determined if the nucleons have definite orbital angular momentum. We write the nucleon wave function in terms of its radial wave function,

$$U_{iL}(\vec{y}) = U_{iL}(y) \sum_{\sigma} Y_{L,\, m+\sigma}(\hat{y}) \chi_m^{\sigma} \quad (25)$$

with

$$\sum_{\sigma} \chi_m^{\sigma\dagger} \chi_m^{\sigma} = 1$$

and

$$\int_0^{\infty} dr\, r^2 |U_{iL}(r)|^2 = 1 .$$

After some manipulation the transition rate can be written simply in terms of a radial overlap function. The transition rate is given by

$$\Gamma = \sum_{Y\pi} \sum_i \sum_J \int_0^{\infty} dp \frac{(2J+1)}{2\pi^2} \left| \begin{pmatrix} J & l & L \\ 0 & 0 & 0 \end{pmatrix} \right|^2 \times p^2 |Z_{iJ}(p)|^2 \left[\frac{W_i k^f_{c.m.}(W_i)}{E_{nl} M_N} \sigma_{K^- i \to Y\pi}(W_i) \right] \quad (26)$$

with the radial overlap function $Z_{iJ}(p)$ defined by

$$Z_{iJ}(p) = \int_0^{\infty} dr\, r^2 j_J(pr) U_{iL}(r) R_{nl}(r) . \quad (27)$$

Recall that the energy available in the center of mass, W_i, was given by

$$W_i \simeq M_K + M_i - \epsilon_{nl} - \epsilon_i - p^2/2W_i . \quad (28)$$

Note that we have essentially diagonalized the magnitude of the momentum, p, as well as keeping an explicit sum over the final states, $Y\pi$. Hence we can use the formula in Eq. (26) to calculate momentum distributions for transitions to definite final states as well as the total absorption rates.

Although occurring in a region of low nuclear density, absorption largely takes place within the range of the nuclear forces, not in the asymptotic tail of the nuclear distribution. Thus we expect (and find) that except for the most tightly bound states, all states make nonnegligible contributions to the absorption rate. This has the important effect of lowering the over-all range of the K-nucleon center-of-mass energy well below that expected for the most lightly bound nucleons. With these considerations, it is essential to use a realistic nuclear model to generate the nucleon wave functions.

Transition rates for K^- absorption determined by Eqs. (26) and (27) were calculated using single-particle wave functions numerically generated for a Woods-Saxon-well potential with Thomas spin-orbit and Coulombic terms[16, 17]:

$$V(r) = -V_{\epsilon} f(r) + V_{s\epsilon} \left(\frac{\hbar}{m_{\pi} c} \right)^2 \frac{1}{r} \frac{df(r)}{dr} \vec{L} \cdot \vec{\sigma} + V_C(r) , \quad (29)$$

where

$$f(r) = [e^{(r-R)/a} + 1]^{-1}$$

and

$$R = r_0 (A-1)^{1/3} .$$

The Coulombic potential V_C is that due to a uniformly charged sphere with radius R. In order to make comparison with x-ray, emulsion, and bubble-chamber studies, three nuclei were investigated – ^{16}O, ^{40}Ca, and ^{96}Mo. For ^{16}O and ^{40}Ca, potential parameters fitting electron-scattering and binding-energy data by Swift and Elton[17] were used. For ^{96}Mo we used the average potential parameters given by Bohr and Mottelson.[18] The parameters we used are listed in Table I. Calculations for these nuclei were based on both the description of the K-nucleon interaction obtained by Martin and Sakitt[15] and by Kim[14] (discussed in more detail in the Appendix). The results of these calculations are discussed in the following sections.

TABLE I. Shell-model potential parameters.

Nucleus	States	V_{ϵ} (MeV)	$V_{s\epsilon}$ (MeV)	r_0 (F)	a (F)
^{16}O	$1s$	68	•••	1.41	0.65
	$1p$	52	13	1.41	0.65
^{40}Ca	$1s$	85	•••	1.30	0.60
	$1p$	60	30	1.30	0.60
	$1d, 2s$	53	12	1.30	0.60
^{96}Mo	proton	55.5	9.85	1.27	0.67
	neutron	47.2	8.37	1.27	0.67

V. COMPARISON WITH X-RAY RESULTS

The total absorption of K mesons in nuclei can be studied by an analysis of the x rays emitted in the electronic cascade of the K-mesonic atoms. Measurements of the x-ray spectra of K-mesonic atoms have been reported by Burleson,[19] by Wiegand and Mack,[20] and by Wiegand.[21] Our analysis is relevant to an analysis of the detailed nuclear-series study made by Wiegand.

The experiments can measure the energy-level shift and the line intensity of the electronic transitions. The intensity measurements can be expressed in terms of a relative yield, $Y(n \to n')$, defined as the ratio of the number of x rays for the

transition $n \to n'$ to the number of x-ray transitions observed filling the level n, where n is the principle quantum number. The relative yield is given by

$$Y(n \to n') = \Gamma_{\text{obs}}(n \to n') / \sum_m \Gamma_{\text{obs}}(m \to n) . \tag{30}$$

The theoretical analysis of the x-ray spectra depends upon the conjecture that the K mesons which survive to the lower electronic orbits will tend to be trapped in circular orbits $n = l + 1$. The radiation rates from circular orbits are easily calculated. Assuming that the K mesons are predominately in circular orbits, the relative yields for circular orbit transitions $(l+1, l) \to (l, l-1)$ can be related to the absorption rate from the state $(l+1, l)$ by the formula

$$Y((l+1, l) \to (l, l-1)) = \frac{\Gamma_{\text{rad}}((l+1, l) \to (l, l-1))}{\Gamma_{\text{rad}}((l+1, l) \to (l, l-1)) + \Gamma_{\text{abs}}(l+1, l)} . \tag{31}$$

The radiation rates for the transition $(l+1, l) \to (l, l-1)$ were calculated using

$$\Gamma_{\text{rad}}((l+1, l) \to (l, l-1)) = \tfrac{2}{3}\alpha(Z\alpha)^4 \frac{(2l+1)^3}{(l+1)^5(2l)^3}\left[\frac{4l(l+1)}{(2l+1)^2}\right]^{2l+3} \tag{32}$$

We have used the theory discussed in Secs. III and IV to calculate Γ_{abs} for the three nuclei ^{16}O, ^{40}Ca, and ^{96}Mo. The results of our calculation are given in Table II; the experimental values are taken from Wiegand.[21] The predictions are the right order of magnitude and quite accurate in the case of Mo. We note that the Mo measurement was the longest cascade series reported by Wiegand.

In addition to the direct comparison of our calculations of the absorption rates with experiment, we can consider calculations in terms of an energy averaging of the production cross sections. The absorption rates are then proportional to the overlap of the K-meson wave function with the nuclear densities in the surface as in Eq. (21). Since the overlap is extremely sensitive to the size and shape of the nuclear density in the surface, we expect the independent-particle calculation of the energy-averaged production cross sections to be more reliable than the actual calculation of the absorption rates. Hence, we use our calculations to define an effective optical-potential strength, $2\overline{W}$. Comparing with the pseudopotential-rate formula in Eq. (8), we define $2\overline{W}$ as

$$2\overline{W}_i = 4\pi\hbar\Gamma_i \Big/ \int d^3x\, \rho_i(\vec{x}) |R_{nl}(x)|^2 . \tag{33}$$

The effective $2\overline{W}$ values for neutrons and protons for the three nuclei studied are given in Table III.

We observe that $2\overline{W}$ is only slowly varying over the range of nuclei studied. Hence, we expect the use of a constant value of $2\overline{W}$ over a wide range of moderate to heavy nuclei to be a good approximation. We have used the following average values of $2\overline{W}$,

Kim:

$$2\overline{W}_p = 3440 \text{ MeV fm}^3, \quad 2\overline{W}_n = 710 \text{ MeV fm}^3 ; \tag{34}$$

Martin and Sakitt:

$$2\overline{W}_p = 2370 \text{ MeV fm}^3, \quad 2\overline{W}_n = 610 \text{ MeV fm}^3 ;$$

and a Fermi-function fit to the nuclear densities to compute the relative x-ray yields for stable nuclei as a function of the charge Z. The neutron and proton densities were taken as[22]

$$\rho(r) = \rho(0)[e^{(r-R)/a} + 1]^{-1} \tag{35}$$

with

$$R = (1.18A^{1/3} - 0.48) \text{ F}$$

and

$$a = 0.55 \text{ F} .$$

Our predictions are compared with the experimental points of Wiegand[21] in Fig. 4. The agreement is good within the large experimental errors; the only serious discrepancy appears to be for lead. A similar qualitative agreement was obtained by Ericson[12] using the smaller threshold values of $2\overline{W}$.

From the pseudopotential parameters and the ratios of absorption rates on protons and neutrons listed in Table III, we see that absorption on protons well exceeds absorption on neutrons. Since the study of x-ray emissions does not distinguish between these channels, it represents an insensitive probe of the neutron distribution. In Fig. 4, we also plot the yields calculated using the above pseudopotential parameters with the neutron density in the periphery enhanced by a factor of 3. The yields are seen to be very insensitive to large changes in the neutron densities. Thus in order to probe the neutron densities using x-ray studies, extremely accurate predictions for the proton

TABLE II. X-ray yields.

	$Y((l+1, l) \to (l, l-1))$			$Y((l+2, l+1) \to (l+1, l))$		
		Th			Th	
	Expt	Kim	MS	Expt[a]	Kim	MS
^{16}O($l=2$)	•••	0.01	0.01	•••	0.91	0.94
^{40}Ca($l=3$)	•••	0.03	0.04	0.6±0.2	0.90	0.92
^{96}Mo($l=4$)	•••	0.01	0.02	0.5±0.2	0.59	0.66

[a] See Ref. 21.

TABLE III. Effective values of $2\overline{W}$.

	$2\overline{W}_p$(MeV fm^3)		$2\overline{W}_n$(MeV fm^3)		$\Gamma(p)/\Gamma(n)$		
	Kim	MS	Kim	MS	Kim	MS	$Z\overline{\rho}_n/N\overline{\rho}_p$
$^{16}O(l=2)$	3430	2240	710	610	5.1	3.9	1.06
$^{40}Ca(l=3)$	3390	2420	700	590	6.2	5.3	1.14
$^{96}Mo(l=4)$	3510	2450	730	640	3.0	2.3	1.26

absorption rates are required. From the standpoint of the ambiguity in the scattering amplitudes alone, the discrepancy between the proton pseudopotential parameters obtained from the fits of Martin and Sakitt and of Kim being larger than the neutron parameter, this is not possible at present.

Another problem caused by the resonance enhancement of the scattering amplitudes concerns the analysis of the initial-state interactions. A qualitative picture can be obtained by considering the pseudopotential analysis in Eqs. (6) and (4). From the fits to the scattering in Fig. 2, we find that both the real and imaginary parts of the pseudopotential are large and can cause distortion of the K-meson wave function. The large imaginary part of the pseudopotential will tend to cause a reduction of the wave function due to absorption. In the energy region where absorption predominately occurs, $W=1400$ to 1420 MeV, the real part of the pseudopotential is attractive, which will tend to increase the wave function in the overlap region. The balance of these effects will determine whether the initial-state interactions have a significant effect on our calculation of the absorption rates. A quantative treatment of the initial-state interactions is difficult. As we have noted, the pseudopotential calculations are unreliable because of the strong energy dependence of the scattering amplitudes. Hence an approach which can take into account the large energy-dependent amplitude must be used. A generalization of the effective t-matrix method to a multiple-scattering t-matrix approach is perhaps feasible.[23]

The initial-state interactions make any predictions of the energy-level shifts extremely unreliable. The pseudopotential predictions can be estimated using Eq. (8). Referring again to the fits to the scattering amplitudes in Fig. 2, we see that the real part of the neutron pseudopotential is small while the presence of the resonance causes the real part of the proton pseudopotential to be large and change sign in the energy region where absorption occurs. Hence, the pseudopotential does not even provide a qualitative estimate of energy-level shifts in K-mesonic atoms.

Finally, the agreement of our calculation of the momenta distributions in Sec. VI with experiment indicates that the final-state interactions should have only a small effect on calculations of the total absorption rates. The effects of final-state interactions are more fully discussed in the following section.

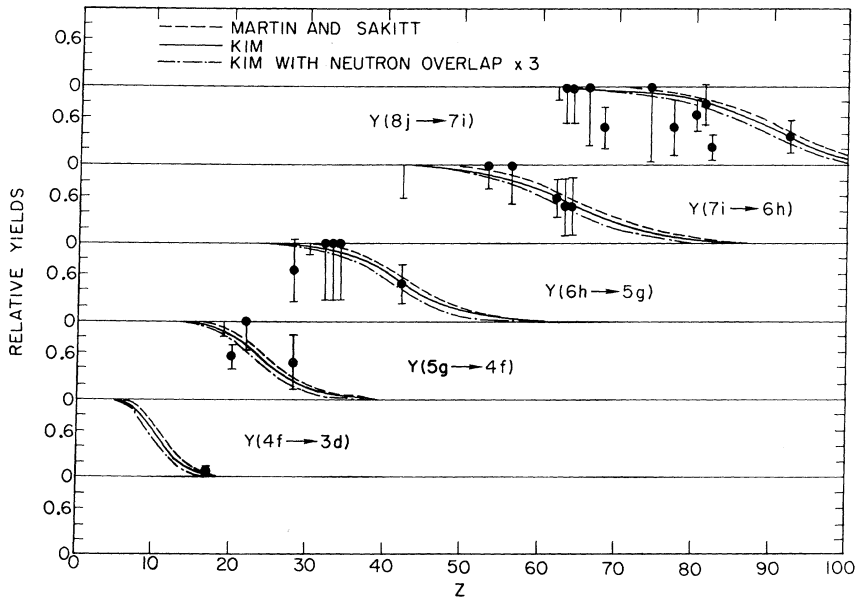

FIG. 4. Observed and calculated relative x-ray yields.

VI. COMPARISON WITH EMULSION AND BUBBLE-CHAMBER RESULTS

In contrast to x-ray data, nuclear emulsion and bubble-chamber studies of the decay of K-mesonic atoms provide detailed data on absorption products and differentiate the absorption channels yielding information such as momentum and opening angle distributions for these products and various branching ratios among these channels. Although lacking the selectivity over the absorption nucleus present in x-ray studies, investigations in emulsions can distinguish between captures on light nuclei (typically a mixture of C, N, and O) and heavy nuclei (Ag and Br), thereby indicating some general features of the Z dependence of the capture process. In the section, we compare these experimental results with predictions based on the independent-particle shell-model approach discussed in Sec. IV.

The total momentum distribution for a given hyperon-pion pair resulting from capture of a K meson with angular momentum l is calculated using Eqs. (26) and (27). As shown in Fig. 5 for ^{40}Ca, the predominant feature of this distribution is a peak matching that given by Eq. (11) but considerably broadened and somewhat displaced to higher momentum by the angular momentum of the nucleons and slightly shifted by the energy dependence of the amplitudes. Since the position of the peak is only weakly dependent on l and Z, the total momentum distribution is relatively insensitive to the precise capture orbit and the composition of the nucleus (see Fig. 6).

Opening-angle distributions for hyperon-pion pairs are directly calculated from the total momentum distribution using the relation

$$\frac{d\Gamma}{d(\cos\alpha)}(\cos\alpha) = \int_0^\infty dP \frac{d^2\Gamma}{dP\,d(\cos\theta)} \frac{d(\cos\theta)}{d(\cos\alpha)}\,, \tag{36}$$

where α denotes the opening angle and θ the angle between the direction of motion of the center of mass and the direction of the emitted pion in the center-of-mass frame. The S-wave dominance of the K-nucleon interaction then allows us to replace the first factor in the integrand by $\frac{1}{2}d\Gamma/dP$. The second factor is a function of P and $\cos\alpha$ and is determined by the Lorentz transformation connecting the laboratory frame to the center-of-mass frame.

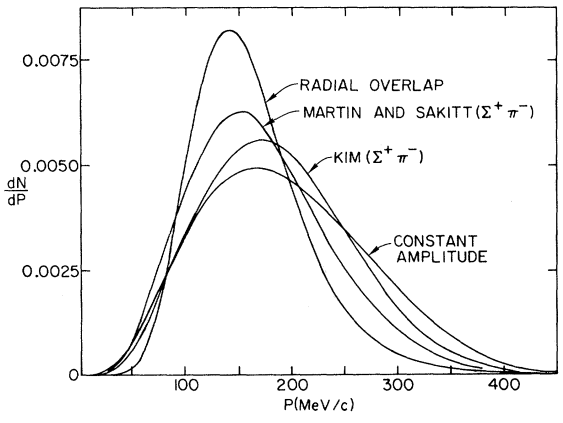

FIG. 5. Total momentum distributions for ^{40}Ca. The radial overlap distribution was calculated from Eq. (11) with $l=3$ and $1/2\beta = 0.576$ F. The constant amplitude distribution corresponds to using an energy-independent amplitude in the independent-particle shell-model calculation.

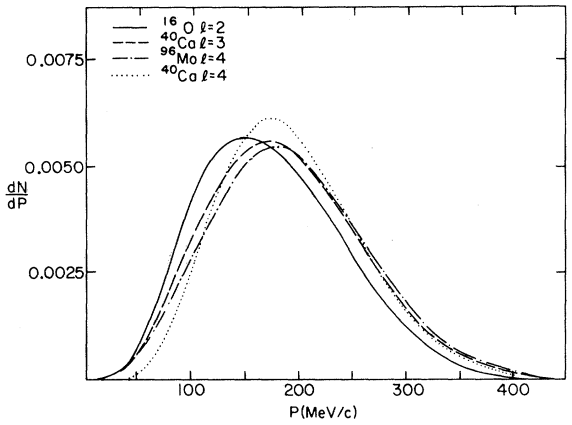

FIG. 6. Calculated total momentum distributions of $\Sigma^+\pi^-$ pairs for selected nuclei and l values based on the Kim amplitudes.

Total momentum and opening-angle distributions of $\Sigma^+\pi^-$ and $\Sigma^-\pi^+$ pairs calculated for ^{16}O($l=2$) and ^{96}Mo($l=4$) are compared in Figs. 7 and 8 with those observed in nuclear emulsions by Lovell and Schorochoff.[24] Over-all agreement is quite good, especially in comparison with the ambiguity in the amplitudes. On the basis of this agreement, we conclude that final-state interactions, which were neglected in the above calculations, are probably weak. The calculated momentum distributions may be displaced by no more than about 30 MeV without appreciably altering the agreement with observation. This corresponds to a total effective final-state interaction potential of less than about 2 MeV. We anticipate that in addition to being absorptive, the final-state interactions will be largely attractive, shifting the momentum distribution towards lower momentum values and the opening-angle distributions towards 180°. These effects will tend to improve the fit for distributions based on Kim amplitudes.

Investigation of appropriate branching ratios among the capture products is a direct means of

determining the neutron-to-proton ratio in the capture region. With this in mind, nuclear emulsion and bubble-chamber studies[7,8,24] have examined the branching ratios E_1 and E_2:

$$E_1 = [N(\Sigma^+\pi^-) + N(\Sigma^-\pi^+)]/N(\Sigma^-\pi^0),$$
$$E_2 = N(\Sigma^+\pi^-)/N(\Sigma^-\pi^+). \quad (37)$$

E_1 provides a measure of the proton-to-neutron density ratio in the absorption region, since $\Sigma^+\pi^-$ and $\Sigma^-\pi^+$ pairs originate from capture on protons and $\Sigma^-\pi^0$ pairs from capture on neutrons. The interpretation of such measurements, however, is complicated by the pronounced energy dependence of the corresponding ratios of production amplitudes R_1 and R_2 shown in Fig. 9.

Table IV lists observed and calculated values for E_1 and E_2, where the heavy-liquid bubble-chamber (HLBC) results describe absorption on light nuclei, the emulsion results differentiate between heavy and light nuclei, and the calculated values correspond to $^{16}O(l=2)$ and $^{96}Mo(l=4)$. The calculated and experimental values are only in qualitative agreement. The calculated value of the ratio E_1 is too low for the light nuclear sample and too high for the heavy nuclear sample. The theoretical values for the ratio E_2 appear to be too large, particularly the estimates based on the Martin and Sakitt amplitudes. Unlike the previous results, the observed branching ratios can be significantly affected by final-state interactions. Although, as pointed out above, the shifts in the average center-of-mass energy due to the final-state interactions is expected to be small, the production cross sections are more rapidly varying than the total absorption amplitude, and the energy averaging can be quite different in the different production channels.

Although detailed analysis of final-state interactions is probably needed to definitively compare calculated and observed branching ratios, several qualitative features of the comparison given in Table IV may be pointed out. First, the very large discrepancy between the values of E_2 based on the Martin and Sakitt amplitudes and the observed values suggests that the zero-range fit may not be adequate for describing the K-proton interaction at energies well below threshold. Second, the relative difference between E_2 for light nuclei and that for heavy nuclei is somewhat larger than predicted using both Martin and Sakitt amplitudes and Kim amplitudes. The calculated values for light and heavy nuclei are nearly the same, reflecting the cancellation of a decrease in average binding energy from light to heavy nuclei by an increase in average kinetic energy due to the

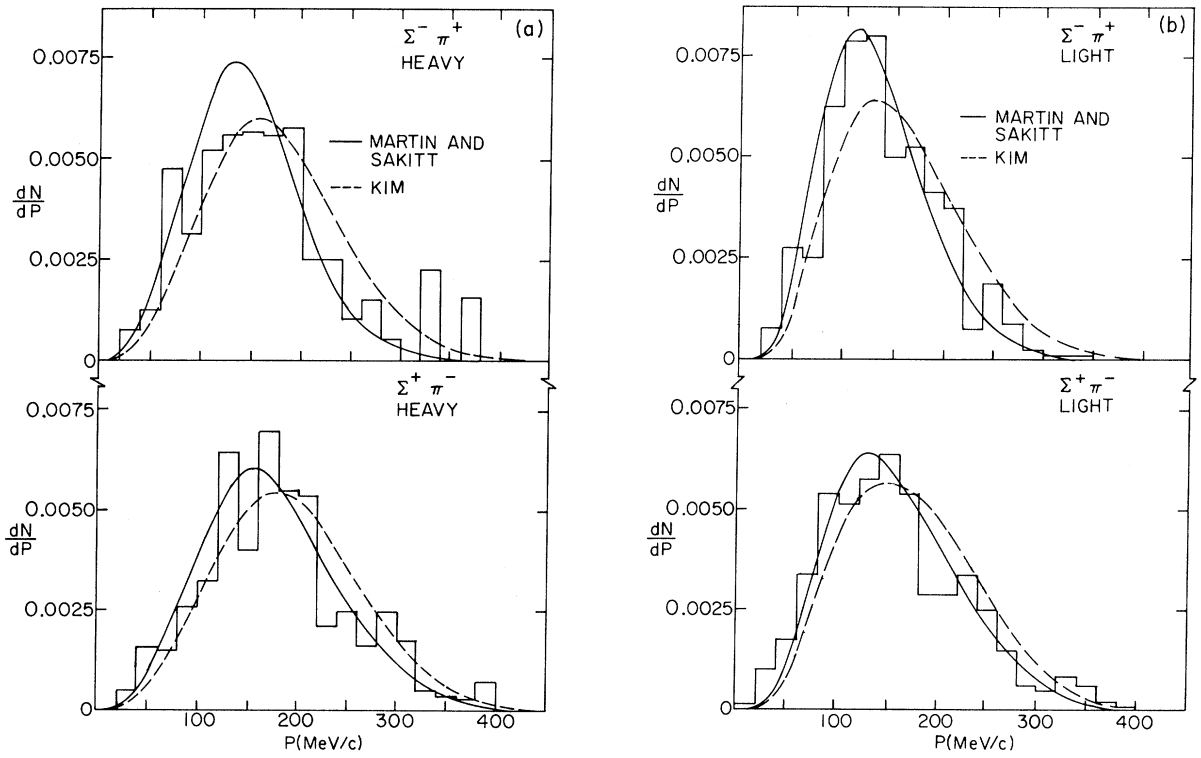

FIG. 7. Observed (histograms) and calculated total momentum distributions of $\Sigma^+\pi^-$ and $\Sigma^-\pi^+$ pairs for heavy (a) and light (b) nuclei.

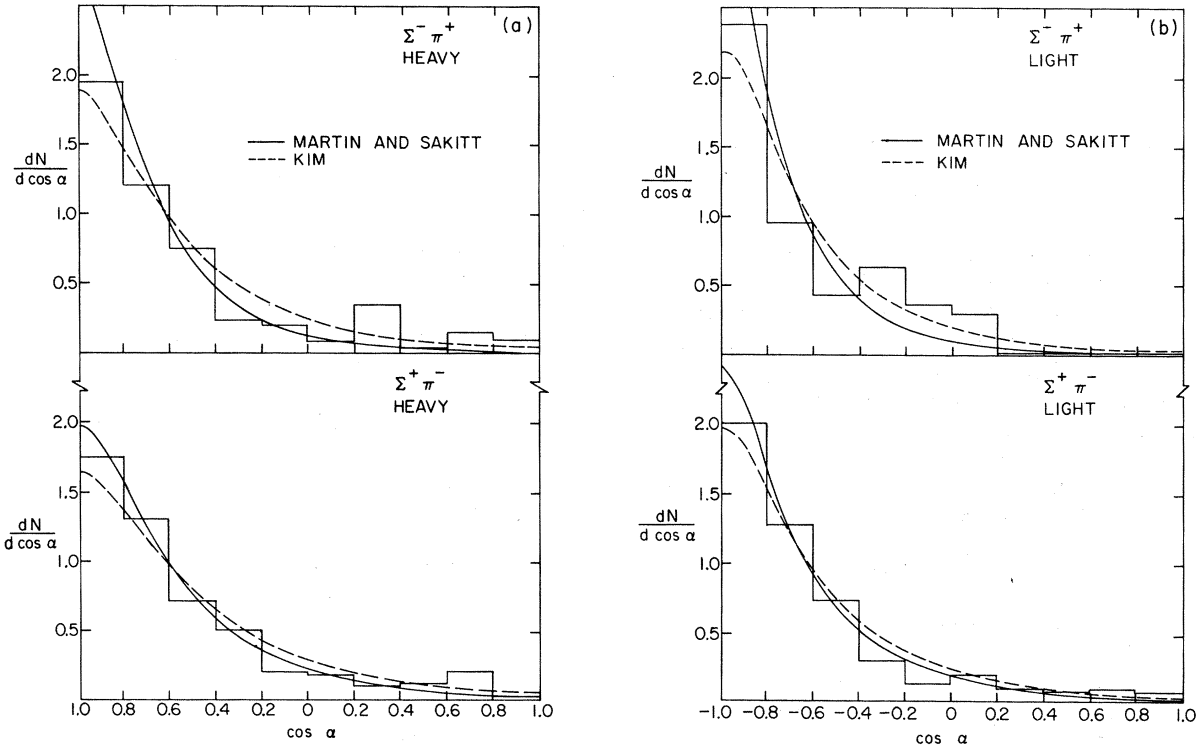

FIG. 8. Observed (histograms) and calculated opening angle distributions of $\Sigma^+\pi^-$ and $\Sigma^-\pi^+$ pairs for heavy (a) and light (b) nuclei.

greater angular momentum of the K meson in heavier nuclei. We note that the average nucleon binding energy is substantially more than the smallest binding energy for both light and heavy nuclei, since absorption occurs where the nuclear potential is still large and where all nuclear states are still important. If we assume that these energy considerations are properly handled by the independent-particle shell model, we would conclude that final-state interactions have appreciably different effects in light and heavy nuclei. Third,

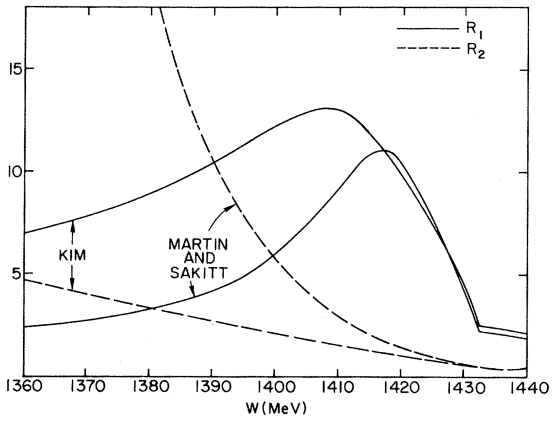

FIG. 9. Dependence of the cross-section ratios R_1 and R_2 on the K-proton center-of-mass energy.

following the analysis of Davis *et al.*,[7] we consider the ratio E_1(light nuclei) to E_1(heavy nuclei). For both Martin and Sakitt and Kim amplitudes, this ratio is close to 2, in contrast to the experimental value of 4.5. Note that the independent-particle shell-model wave functions predict a neutron excess in the absorption region of 20% for ^{96}Mo over ^{16}O as given in Table III. Thus, the neutron excess implied by the experimental value is considerably reduced. Finally, the observed value of E_1 (light nuclei) greatly exceeds the maximum value of R_1 given in Fig. 9. The average energies for the various channels are actually different, permitting values for E_1 larger than this maximum value. But since the neutron amplitudes are only weakly dependent on energy, E_1 should not be significantly larger than the maximum value of R_1, at worst. Thus, unless final-state interactions strongly favor absorption of products for capture on neutrons versus products for capture on protons, the experimental value of E_1(light nuclei) is probably excessive. This suggests a further reduction in the observed neutron excess.

The interpretation of the emulsion results can also be strongly affected by observational bias introduced in the separation of the absorption on light and heavy nuclei. The observation of the track of the recoil nucleus is used as the signature of absorption on light nuclei. This signature will

TABLE IV. Branching ratios.

	E_1			E_2		
	Expt	Th (Kim)	Th (MS)	Expt	Th (Kim)	Th (MS)
HLBC	20.7 ± 6.9	12.9	7.8	1.4 ± 0.3	1.85	3.6
EM (light)	22.4 ± 4.4	12.9	7.8	1.73 ± 0.17	1.85	3.6
EM (heavy)	4.5 ± 0.6	7.2	4.7	1.19 ± 0.13	1.75	3.1

introduce a bias against Σ, π pairs with low total momentum of the center of mass. If this effect is large, we would have to increase the number of observed Σ, π pairs with low momentum to compare with our theoretical curves in Fig. 7(b). As the experimental momentum distribution would then tend to peak at lower momenta than the calculated curves, we might expect the final-state interactions to play a larger role than indicated in the previous discussion.

VII. CONCLUSIONS

The absorption process in K-mesonic atoms is severely complicated by the existence of the $Y_0^*(1405)$ resonance. Our estimates of the energy available in the center of mass of the K-nucleon system during absorption show that absorption occurs well below the free-particle threshold in a broad region surrounding the resonance.

The resonance causes a large enhancement of the absorption on protons. Hence, x-ray studies, which do not differentiate the final states, are insensitive probes of neutron distributions in nuclei. The energy dependence of the production amplitudes further complicates the analysis of absorption on protons. However, on the basis of the effective t-matrix calculations, we do find it possible to define effective energy-independent pseudopotential parameters to describe the absorption. We obtain good qualitative, perhaps quantitative, agreement with the x-ray yields for a wide range of moderate to heavy nuclei. On the other hand, the theory cannot make any reliable estimates of the energy shifts due to the rapid variation of the real part of the pseudopotential. More-precise studies, such as needed to extract information about neutron distributions, are complicated by the ambiguities in the extrapolation of the K-nucleon production amplitudes below threshold and by the effects of initial-state interactions.

The emulsion experiments which can differentiate the final states are also not currently clean probes of the neutron distributions. The theoretical analysis is complicated by the possibility of important final-state interactions in addition to the ambiguity associated with the extrapolation of the various production amplitudes. There may also be important observational bias introduced in the separation of absorption on heavy and light nuclei which can affect the interpretation of the experimental results. The predictions of the effective t-matrix method combined with the independent-particle model for the nucleus show only qualitative agreement with the emulsion results. Whether the emulsion experiments can be used to probe the nucleus must await a better understanding of both theory and experiment.

Note added in proof: We wish to acknowledge a recent paper by Bloom, Johnson, and Teller,[25] which reviews the K-meson absorption process including the role of the Y_0^* resonance.

ACKNOWLEDGMENTS

We would like to thank Professor Dirk Walecka for his initial participation in this research and for his continuing interest and encouragement. We would also like to thank Dr. Frank Dietrich for the use of his computer program SCHRO.

APPENDIX

K-Nucleon Amplitudes

Fits to K^--p scattering data by Martin and Sakitt[15] and by Kim[14] are based on the multichannel K-matrix analysis formulated by Dalitz and Tuan.[26] Under this description, the t matrix is given in terms of a real, symmetric matrix K by

$$T = (K^{-1} - ik)^{-1},$$

where k is the diagonal matrix of center-of-mass channel momenta. Martin and Sakitt use the zero-range approximation in which K is taken to be energy independent, while Kim applies the effective-range method proposed by Ross and Shaw[27] in which

$$K^{-1} = M(E_0) + R(k^2 - k_0^2),$$

where $M(E_0)$ and R are energy independent and R is diagonal.

Using average masses in computing the effective-range contribution for Kim's fit, the K matrices obtained from parameters given by Martin and Sakitt and by Kim are diagonal with respect to I and independent of I_z. In order to treat the mass differences between states of definite charge, the K matrix was transformed by a rotation in isospin

space from states with definite I and I_z to states with definite charge. Then, the ik term was evaluated using the masses appropriate to these latter states. In actuality, the effect of these mass differences is minimal in the present calculations, since the absorption of the K meson occurs predominantly at energies well away from any channel threshold.

---

*Research sponsored by the Air Force Office of Scientific Research, Office of Aerospace Research, U. S. Air Force.

†National Science Foundation Predoctoral Fellow.

[1]J. D. Walecka, in *High-Energy Physics and Nuclear Structure,* edited by S. Devons (Plenum Press, Inc., New York, 1970), p.1.

[2]R. Engfer, in *High-Energy Physics and Nuclear Structure,* edited by S. Devons (Plenum Press, Inc., New York, 1970) p. 104.

[3]E. H. S. Burhop, in *High-Energy Physics,* edited by E. H. S. Burhop (Academic Press Inc., New York, 1969), p. 110.

[4]D. H. Wilkinson, Phil. Mag. 4, 215 (1959).

[5]P. B. Jones, Phil. Mag. 3, 33 (1958).

[6]Y. Eisenberg and D. Kessler, Phys. Rev. 130, 2352 (1963); A. D. Martin, Nuovo Cimento 27, 1359 (1963).

[7]D. H. Davis, S. P. Lovell, M. Csejthey-Barth, J. Sacton, G. Schorochoff, and M. O'Reilly, Nucl. Phys. B1, 434 (1967).

[8]E. H. S. Burhop, Nucl. Phys. B1, 438 (1967).

[9]E. H. S. Burhop, D. H. Davis, J. Sacton, and G. Schorochoff, Nucl. Phys. A132, 625 (1969).

[10]C. E. Wiegand, in *High-Energy Physics and Nuclear Structure,* edited by S. Devons (Plenum Press, Inc., New York, 1970), p. 502.

[11]W. M. Bugg, G. T. Condo, H. O. Cohn, and R. D. Hill, Nucl. Phys. A124, 212 (1969).

[12]T. E. O. Ericson and F. Scheck, Nucl. Phys. B19, 450 (1970).

[13]S. D. Bloom, M. H. Johnson, and E. Teller, Phys. Rev. Letters 23, 28 (1969).

[14]J. K. Kim, Phys. Rev. Letters 19, 1074 (1967).

[15]B. R. Martin and M. Sakitt, Phys. Rev. 183, 1345 (1969).

[16]The shell-model wave functions were computed using a program, SCHRO, supplied by F. Dietrich, private communication.

[17]L. R. B. Elton and A. Swift, Nucl. Phys. A94, 52 (1967).

[18]A. Bohr and B. R. Mottelson, *Nuclear Structure* (W. A. Benjamin, Inc., New York, 1969), Vol. I, pp. 236–240.

[19]G. R. Burleson, D. Cohen, R. C. Lamb, D. N. Michael, R. A. Schluter, and T. O. White, Phys. Rev. Letters 15, 70 (1965).

[20]C. E. Wiegand and D. A. Mack, Phys. Rev. Letters 18, 685 (1967).

[21]C. E. Wiegand, Phys. Rev. Letters 22, 1235 (1969).

[22]R. Hofstadter and H. R. Collard, in *Landolt-Börnstein,* edited by K. H. Hellwege (Springer-Verlag, New York, 1967), Group I, Vol. 2, p. 21.

[23]We understand that R. Seki has made some preliminary calculations comparing "exact" and perturbation treatments of the initial-state interactions, private communication.

[24]S. P. Lovell and G. Schorochoff, Nucl. Phys. B5, 381 (1968).

[25]S. D. Bloom, M. Johnson, and E. Teller, University of California Radiation Laboratory Report No. UCRL-72807 (unpublished).

[26]R. Dalitz and S. Tuan, Ann. Phys. (N.Y.) 10, 307 (1960).

[27]M. Ross and G. Shaw, Ann. Phys. (N.Y.) 13, 147 (1961).